

# Exosomes from myoblasts induced by hypoxic preconditioning improved ventricular conduction by increasing Cx43 expression in hypothermia ischemia reperfusion hearts

**Tingju Hu**

Soochow University School of Medicine

**Hong Gao** (✉ [18798000325@163.com](mailto:18798000325@163.com))

Guizhou Hospital of the First Affiliated Hospital of Sun Yat-sen University

**Rui Duan**

the Second People's Hospital of Guiyang

**Xue Bai**

Guizhou Medical University

**Xiang Huang**

Guizhou Medical University

**Xu Yan**

Guizhou Medical University

**Li An**

Guizhou Medical University

**Yanyan Ma**

Guizhou Medical University

**Rui Chen**

Guizhou Medical University

**Sen Hong**

the Second People's Hospital of Guiyang

**Mi Gan**

Guizhou Medical University

---

## Research Article

**Keywords:** hypoxia preconditioning, exosome, reperfusion arrhythmia, conduction velocity, microelectrode array, Cx43

**Posted Date:** December 6th, 2023

**DOI:** <https://doi.org/10.21203/rs.3.rs-3700347/v1>

**License:**  This work is licensed under a Creative Commons Attribution 4.0 International License.

[Read Full License](#)

**Additional Declarations:** No competing interests reported.

---

# Abstract

Myocardial ischemia-reperfusion arrhythmia after cardiac surgery is common and seriously affects quality of life. Remote ischemic preconditioning can reduce the myocardial damage caused by severe ischemia. However, the underlying mechanism is not well understood. This study aimed to investigate the effects of exosomes derived from C2C12 mouse myoblasts after hypoxic preconditioning (HP) on ventricular conduction in hypothermic ischemia-reperfusion hearts. Myocardial ischemia-reperfusion model rats were established using the Langendorff cardiac perfusion system. Exosomes derived from normoxic (ExoA) and hypoxia-preconditioned (ExoB) C2C12 cells were injected into the jugular vein of the model rats. The time to heartbeat restoration, arrhythmia type and duration, and heart rate were recorded after myocardial ischemia-reperfusion. Conduction velocity on the surface of left ventricle was measured using a microelectrode array after 30 min of balanced perfusion, 15 min of reperfusion, and 30 min of reperfusion. Immunofluorescence and western blotting were performed to determine the distribution and relative expression of connexin 43 (Cx43). ExoB contained more exosomes than ExoA, showing that HP stimulated the release of exosomes. The IR + ExoB group showed faster recovery of ventricular myocardial activity, a lower arrhythmia score, faster conduction velocity, and better electrical conductivity than the IR group. ExoB increased the expression of Cx43 and reduced its lateralization in the ventricular muscle. Our study showed that exosomes induced by hypoxic preconditioning can improve ventricular myocardial conduction and reperfusion arrhythmia in isolated hearts after hypothermic ischemia-reperfusion.

## Introduction

Open heart surgery is the main clinical treatment for valvular heart disease, coronary heart disease, and other cardiovascular diseases. During open heart surgery, the myocardium undergoes ischemia and recovery perfusion, which generates a large number of oxygen free radicals and inflammatory factors, leading to calcium overload and other factors. These physiopathological changes cause cardiomyocyte damage and dysfunction, which is called myocardial ischemia-reperfusion injury (MIRI) (GAO et al. 2021). The clinical manifestations of MIRI (DAVIDSON et al. 2019; Ibáñez et al. 2015; KULEK et al. 2020) include reperfusion arrhythmia (RA), myocardial depression, and microvascular obstruction. The incidence of RA is as high as 85% (KADRIC and OSMANOVIC 2017). Its main manifestations include premature ventricular beats, ventricular tachycardia (VT), and ventricular fibrillation. RA can cause heart failure and cardiogenic shock during the postoperative period and can trigger hemodynamic disorders and even lead to sudden cardiac death (SCD) (BERNIKOVA et al. 2018; GONCA 2015; PATIL et al. 2015). Although RA has a severe impact on patient prognosis, there are no prevention strategies. Therefore, clinically relevant measures are urgently needed to address this issue.

Remote ischemic preconditioning has been shown to protect the myocardium against the damage caused by severe ischemia. Przyklenk et al. (1993) showed that transient and multiple ischemic treatments on the left branch of the coronary artery in dogs significantly decreased the area of myocardial infarction. Kharbanda et al. (2002) extended the concept of remote ischemic preconditioning

(RIPC) to tissues far from the heart, by showing that brief and repeated ischemic preconditioning can reduce the myocardial damage caused by severe ischemia. Subsequent studies have shown that even limb ischemic preconditioning has a protective effect against myocardial ischemia-reperfusion injury (CHO and KIM 2019; AMANAKIS et al. 2019; YAN et al. 2021) and improves myocardial ischemia-reperfusion arrhythmia (AMANAKIS et al. 2019; YAN et al. 2021; KINDERNAY et al. 2021; OXMAN et al. 1997). Although ischemic preconditioning appears to be a powerful myocardial protective intervention, its clinical application has been largely disappointing (KLEINBONGARD et al. 2020). Which cardioprotective factors are transferred from distant organs to the heart during RIPC and the specific mechanisms of action are unknown.

Exosomes are small (30–150 nm in diameter) cellular vesicles produced by cells. Exosomes carry diverse bioactive molecules, including proteins, nucleic acids, and small-molecules. Exosomes fuse with cell membranes in the form of intracellular polyvesicles, which are then released outside the cells. Although exosomes were once considered to be inactive cell fragments, they are now recognized as bioactive entities and have become a research focus. Studies have shown that exosomes are important in intercellular communication and can transfer their internal molecules to distant target cells, and thus participate in a variety of biological processes and cellular functions. Exosomes have been shown to play key roles in cell proliferation, differentiation, migration, and immune regulation by releasing active factors outside the cell. Under physiological conditions, cells can release small amounts of exosomes. However, certain internal and external stimuli, such as hypoxia, signaling pathway activation, and stress (Luo et al. 2023; Minghua et al. 2018; Vicencio et al. 2015; Chen et al. 2022), induce cells to secrete large amounts of exosomes. Donato (Donato et al. 2021) showed that different pretreatment stimulation sites (such as the muscle, mesentery, and kidney) invoke different protective mechanisms involving different substances; Skeletal muscle ischemia pretreatment promotes the secretion of exosomes and miRNAs. Although exosomes have an important protective effect in RIPC in ischemic myocardium (HOU et al. 2019; LUO et al. 2023; MINGHUA et al. 2018), the specific protective mechanism against reperfusion arrhythmia remains unclear and whether and how exosomes are involved is unknown.

Connexin 43 (Cx43) is a transmembrane protein and one of the most abundantly expressed connexin subtypes in the heart. Cx43 plays an important role in the occurrence and development of RA. Previous studies by our research team (Li et al. 2019a; Li et al. 2019b; Yi et al. 2022) and Mahoney et al. (2016) showed that the decrease in ventricular muscle conduction velocity is related to downregulation of Cx43. We also found that abnormal expression, distribution, and phosphorylation of Cx43 in cardiomyocytes can cause RA. Cx43 has been reported to be present on exosome membranes (Ribeiro-Rodrigues et al. 2017; Soares et al. 2015; Cho et al. 2021). Thus, we sought to explore whether Cx43 is involved in RIPC of the myocardium.

A few studies have investigated the role of the exosomes released from HP-treated myoblasts. Thus, skeletal muscle cells are potential candidates for the delivery of exosomes as protective signals during RIPC (YAN et al. 2021). Therefore, we performed cyclic hypoxic preconditioning (HP) of a mouse skeletal muscle myoblast cell line (C2C12) as a cell model for distal limb ischemic preconditioning and used the

Langendorff reperfusion model to simulate the myocardial ischemia-reperfusion process that occurs in clinical cardiopulmonary bypass. In this study, we aimed to investigate the effects of hypoxia-preconditioned C2C12-derived exosomes on ventricular conduction in rats with global heart hypothermia and ischemia-reperfusion and explored the role of Cx43 in the underlying mechanism.

## Materials and methods

### *Cell culture and hypoxic preconditioning*

C2C12 mouse myoblasts were cultured in 10% fetal bovine serum (FBS; Gibco, USA), 1% penicillin-streptomycin (Shanghai Qashipang Biological Technology Shanghai, China), and Dulbecco's modified Eagle's medium (Gibco). The medium was changed every 2 days. Confluence and the growth status of the cells were observed regularly. When the cell reached 70%–80% confluence and were in good condition, the culture medium was discarded, and the cells were washed twice with 5 mL of phosphate buffered saline (PBS). After the addition of 10% exosome-depleted FBS (Shanghai XP Biomed Ltd., Shanghai, China), the cells were randomly divided into two groups: one was cultured for 25.3 h under normoxic conditions in a conventional incubator with 5% CO<sub>2</sub> at 37°C, and the other was cultured under hypoxic conditions in 5% CO<sub>2</sub>, 95% N<sub>2</sub>, and <1% O<sub>2</sub> for 10 min in a three-gas incubator at 37°C, and then reoxygenated for 10 min in conventional incubator at 5% CO<sub>2</sub> at 37°C, to complete a 20 min cycle. After four cycles, the cells were cultured for 24 h. After incubation, the supernatant of the normoxic and hypoxia-treated cells was collected for exosome extraction to generate preparations called ExoA (normoxic) and ExoB (hypoxia-treated), respectively.

### *Extraction, purification, and verification of exosomes*

Exosomes were extracted was using an Exosome Extraction Kit (Umibio, Shanghai, China) according to the manufacturer's instructions. The culture supernatant described in Cell culture and hypoxic preconditioning was centrifuged at 3000 × *g* for 10 min to remove cell debris and then transferred to a new centrifuge tube. ECS exosome extraction solution was then added to the tube. After the mixture was refrigerated at 4°C for 2–16 h to precipitate the exosomes, it was centrifuged at 10000 × *g* for 60 min to sediment the exosomes. The supernatant was discarded, and the exosomes were carefully resuspended in PBS and then centrifuged at 12000 × *g* for 2 min. The supernatant contained exosomes and was transferred to the purification column and centrifuged at 3000 × *g* for 10 min to purify the exosomes. The concentration was determined using a bicinchoninic acid (BCA) kit, and the purified exosomes were aliquoted into 50–100 μL EP tubes and stored at -80°C until use.

The biological and structural characteristics of the exosomes were evaluated using transmission electron microscopy (TEM), Nano Flow cytometry (NanoFCM), and western blotting. TEM: Exosomes (10 μL) and uranyl acetate (10 μL) were mixed and placed on a copper mesh for 1 min and then precipitated for 1 min. The excess liquid was absorbed with a filter paper. Exosomes were analyzed and photographed using a TEM (Hitachi Co., Ltd., Japan). Particle size was analyzed by NanoFCM with a nanoflow analyzer

(Fuliu Biotechnology Co., Ltd., Xiamen, China) using a mixture of exosomes (10  $\mu$ L) that were diluted to 3 fold with PBS (20  $\mu$ L).

### ***Ethical approval***

This study was approved by the Ethics Committee of Guizhou Medical University (Approval number: 2200390). All animal handling and experiments were conducted in accordance with the Guide for the Care and Use of Laboratory Animals of the National Institutes of Health.

The rats were provided by the Animal Experimental Center of Guizhou Medical University [license no. : SCXK (Qian) 2018-0001]. The rats were housed under a 12 h light-dark cycle and were given free access to food and water.

### ***Solutions***

We prepared two solutions as follows: Krebs-Henseleit solution (K-H solution, mmol/L): NaCl, 118; CaCl<sub>2</sub>, 1.26; KCl, 4.5; MgSO<sub>4</sub>·7H<sub>2</sub>O, 1.22; KH<sub>2</sub>PO<sub>4</sub>, 1.18; C<sub>6</sub>H<sub>12</sub>O<sub>6</sub>, 11.1; NaHCO<sub>3</sub>, 24.99, pH 7.35–7.45 and St. Thomas's solution (mmol/L): NaCl, 110; CaCl<sub>2</sub>, 1.26; KCl, 16.1; MgCl, 15.96; KH<sub>2</sub>PO<sub>4</sub>, 1.18; C<sub>6</sub>H<sub>12</sub>O<sub>6</sub>, 11.1; NaHCO<sub>3</sub>, 9.99, pH 7.8 (An et al. 2023 ).

### ***Grouping and establishment of Langendorff perfused heart model rats***

Healthy male SD rats (SPF grade, 8–12 weeks old, weighing 260–320 g) were randomly divided into four groups (n = 8): the control (C), ischemia-reperfusion (IR), ischemia-reperfusion + normoxic C2C12-derived exosome (IR+ExoA), and ischemia-reperfusion + hypoxia preconditioning C2C12-derived exosome (IR+ExoB) groups. The IR+ExoA and IR+ExoB groups were injected with 250  $\mu$ g of ExoA and ExoB, respectively, through the jugular vein at 30 min before ischemia-reperfusion

The rats were injected intraperitoneally with 3% heparin (312.5 U/100 g) for anticoagulation and then with 1% pentobarbital sodium (0.4 mL/100 g) for anesthesia. After the onset of anesthesia, the rats were placed in the supine position, and the thorax was opened to expose the heart. The heart was quickly removed to K-H solution at 4°C. The aorta was fixed using a Langendorff apparatus (HUGO SACHS ELEKTRONIK, Germany). The K-H solution was prefilled with a 95% O<sub>2</sub>-5% CO<sub>2</sub> mixture. Retrograde non-circulating perfusion was performed at constant temperature (37°C) and pressure (8.65 kPa). The criteria for successful model establishment were: the isolated heart recovered a normal beating rhythm and a heart rate  $\geq$ 180 beats /min within 15 min of balanced infusion of K-H solution.

The control group (C) underwent continuous balanced perfusion for 120 min. The IR, IR+ExoA, and IR+ExoB groups underwent balanced perfusion for 30 min. Then, Thomas' solution (at a dose of 2 mL/100 g) was injected into the aortic root. After another 30 min, Thomas' solution was reinjected (at 1 mL/100 g). The heart was protected with K-H at 4°C for 60 min during the ischemia process. They were perfused for 30 min.

### ***Measurement of ventricular conduction velocity using microelectrode array***

After balanced perfusion for 15 min, 64 matrix electrodes were placed on the anterior wall of the left ventricle. The positions of the electrodes were determined by the left anterior descending branch, aorta, and atrium, with channel 1 near the bottom of the heart and channel 64 near the apex of the heart. The electrode was placed at the aortic root, and the electrode lead was connected to the signal input line of the 64-channel MEA mapping system (EMS64-USB-1003; MappingLab Ltd., UK). The local electrical conduction velocity (CV) and conduction activation maps of left ventricle were calculated. The time of heartbeat restoration and the types and durations of arrhythmias during 30 min of reperfusion were recorded as previously described (Ma et al. 2023 Wang et al. 2019). Arrhythmia was scored based on the Lambeth Convention (Walker et al. 1988). The heart rate was recorded at each time point.

After reperfusion, the apex of the heart was immediately fixed with paraformaldehyde (10 g/L) and then stored at 4°C until histological analysis. The remaining left ventricular muscle tissue was frozen at -80°C until subsequent use.

### ***Immunohistochemistry***

Ventricular muscle tissue was fixed with paraformaldehyde solution, decalcified with EDTA, hydrated with ethanol, embedded in paraffin, and cut into slices. The tissue was then soaked in citric acid buffer (0.01 M). The tissue was blocked in 5% bovine serum albumin (BSA) at 37°C for 30 min. Then the tissue was incubated with a primary antibody against Cx43 (1:5000; Abcam, USA) at 4°C overnight. After incubation with the secondary antibody labeled by horseradish peroxidase (1:1000, Beijing Boosen Biotechnology Co., Ltd., China) at 37°C for 30 min, SABC immunohistochemical reagent was added to stain the antibody-protein complexes. DAB color-developing agent and hematoxylin were added and incubated for 2–3 min. Finally, the slices were dehydrated and sealed. The slices were observed under a full-slide optical microscope (OLYMPUS SLIDEVIEW VS200; Shanghai Co., Ltd.).

### ***Western blotting***

The total protein concentration of the myocardial tissue in each group was quantified using a BCA kit. After electrophoresis on a 12% sodium dodecyl sulfate-polyacrylamide gel, the proteins were transferred to PVDF membranes. The membranes were blocked with quick blocking buffer for 15–20 min. After washing, the membranes were incubated with anti-CX43 rabbit and anti-rat primary antibody (1:1000; Abcam) at 4°C overnight with shaking. The next day, the membrane was incubated with an horseradish peroxidase-labeled secondary antibody (1:1000; Beijing Boosen Biotechnology) at room temperature for 1 h with shaking. After incubation, ECL developer was added, and the membrane was imaged using an automatic chemical emission imaging system (Tanon-5200; Shanghai Tianneng Technology Co., Ltd., China). The gray values of each band were analyzed using ImageJ software. Finally, relative protein levels were calculated using GAPDH (1:1000; Bioword Corporation, USA) as a reference.

### ***Hematoxylin and eosin (HE) staining***

After ischemia-reperfusion, left ventricular tissue was fixed with 4% paraformaldehyde, embedded in paraffin, and cut into slices (Leica RM2235; Leica Microsystems Shanghai Co., Ltd.). The slices were then dewaxed with xylene and hydrated with ethanol. The nuclei were stained with hematoxylin, and the cytoplasm was stained with eosin. The sections were dehydrated with alcohol, cleared in xylene, and observed under a microscope.

### ***In vivo Imaging of DiR-labeled exosomes***

To label exosome for imaging, first the fluorescent, lipophilic dye DiR was diluted 10 fold with 1× PBS to prepare a 100 μM working solution, which was mixed with the exosome preparations. The dye working solution and exosomes were mixed for 1 min and then incubated at 37°C for 30 min. Next, 10 mL of 1× PBS was added to the exosome-dye mixture, and the exosomes were extracted using a centrifugal filter device (Amicon Ultra-15 10 K; Millipore, Billerica, MA, USA) to remove excess dye. Finally, the precipitation containing the stained exosomes was resuspended in 200 μL of 1× PBS. Exposure to light was avoided during the entire process.

DiR-labeled exosomes (DiR-exo) were injected into the jugular vein. After administration, rats were anesthetized and placed in the supine position with their limbs facing upward in an imaging box (IVIS Lumina III In Vivo Imaging System; PerkinElmer) In vivo images were obtained at 30 min, 6 h, and 24 h after injection.

### ***Statistical analysis***

Data were analyzed and plotted using GraphPad Prism software (version 9.0). Two independent sample t-tests were used for comparisons between two groups. Analysis of variance (ANOVA) was used to compare multiple groups. Values are expressed as the mean ± standard deviation (SD). Statistical significance was set at  $P < 0.05$ .

## **Results**

### ***Identification and evaluation of exosomes***

TEM showed that the particles in both ExoA and ExoB exhibited classical cup shapes (Fig. 1A and B). NanoFCM showed that the average sizes of the particles in ExoA and ExoB were 71.70 and 74.00 nm, respectively (Fig. 1C and D), and the concentrations were  $8.85E+9$  and  $4.54E+10$  particles/mL, respectively (Fig. 1E and F). These results are consistent with those reported in the literature and confirm successful exosome enrichment. The number of exosomes secreted by the cells two treatments as calculated using nanoFCM showed that the number of particles in ExoB was significantly higher than that in ExoA (Fig. 1G).

**Fig. 1** Identification and analysis of exosomes derived from normoxic (ExoA) and hypoxia-preconditioned (ExoB) C2C12 mouse myoblasts: (A, C, E) normoxic exosomes (ExoA) and (B, D, F) hypoxic-pretreated



exosomes (ExoB). (G) Comparison of particle number between ExoA and ExoB,  $n = 3$ , <sup>a</sup>  $P < 0.05$  vs ExoA

### ***Effects of exosomes on heartbeat restoration time after reperfusion and arrhythmia occurrence within 30 min after reperfusion***

The establishment of the isolated Langendorff myocardial ischemia-reperfusion model is shown in Fig. 2A. During balanced perfusion, there was no significant difference in the time to heartbeat restoration among the four groups (Fig. 2B). During reperfusion, the time to heartbeat restoration in the IR+ExoB and IR+ExoA groups was significantly shorter than that in the IR+ExoB group. The time to heartbeat restoration in the IR+ExoB group was shorter than that in the IR+ExoA group (Fig. 2C).

Arrhythmia scores in the IR+ExoB and IR+ExoA groups were significantly lower than those in the IR group (Fig. 2D). The duration of RA in the IR+ExoB and IR+ExoA groups was significantly lower than that in the IR group, and the duration of RA in the IR+ExoB group was significantly shorter than that in the IR+ExoA group (Fig. 2E).

**Fig. 2** The effects of ExoB and ExoA to reperfusion arrhythmia. (A), Establishment of Langendorff isolated myocardial ischemia-reperfusion model rats (B), and analysis of the effects of exosomes on the time of heartbeat restoration during balanced perfusion (C), the time of heartbeat restoration during reperfusion (D), arrhythmia score (E), and the duration of reperfusion arrhythmia,  $n = 8$ , <sup>a</sup>  $P < 0.05$ , <sup>aaaa</sup>  $P < 0.0001$  vs IR; <sup>b</sup>  $P < 0.05$  vs IR+ExoA

### ***Effects of exosomes on heart rate(HR) at different time points***

HR was measured at four time points: before perfusion ( $T_0$ ), after 30 min of balanced perfusion ( $T_1$ ), after 15 min of reperfusion ( $T_2$ ), and after 30 min of reperfusion ( $T_3$ ). At  $T_0$  and  $T_1$ , there were no statistically significant differences in HR among the four groups (Fig. 3A and B). The HR at  $T_2$  and  $T_3$  in the C, IR+ExoB and IR+ExoA groups was significantly higher than that in the IR group (Fig. 3C and D). The HR at  $T_2$  and  $T_3$  was significantly higher in the IR+ExoB group than in the IR+ExoA group (Fig. 3C and D). Further, the HR in the IR and IR+ExoA groups was significantly lower at  $T_2$  and  $T_3$  than at  $T_1$ . There was no significant difference in the HR between the IR+ExoB and C groups at  $T_2$  and  $T_3$  (Fig. 3E).

**Fig. 3** Effects of exosomes on the heart rate of model rats. (A–D) Heart rate at  $T_0$ ,  $T_1$ ,  $T_2$ , and  $T_3$ ,  $n = 8$ , <sup>a</sup>  $P < 0.05$ , <sup>aaaa</sup>  $P < 0.0001$  vs IR; <sup>b</sup>  $P < 0.05$  vs IR+ExoA, (E) Heart rate of all groups at each time point, <sup>c</sup> IR, <sup>cccc</sup>  $P < 0.0001$  vs  $T_1$ , <sup>d</sup> IR+ExoA, <sup>ddd</sup>  $P < 0.01$ , <sup>dddd</sup>  $P < 0.0001$  vs  $T_1$

### ***Effects of exosomes on conduction velocity (CV) at different time points***

The typical conduction activation maps at  $T_2$  are shown in Fig. 4A. There was no significant change in the CV of the four groups at  $T_1$  (Fig. 4B). The CV at  $T_2$  and  $T_3$  in the C, IR+ExoB, and IR+ExoA groups were significantly higher than those in the IR group. At  $T_2$  and  $T_3$ , the CV of the IR+ExoB group was higher than

those in the IR+ExoA group (Fig. 4C and D). Compared with T<sub>1</sub>, the CV in the IR and IR+ExoA groups was significantly lower at T<sub>2</sub> and T<sub>3</sub>. In the IR+ExoB group, The CV decreased significantly from T<sub>1</sub> to T<sub>2</sub>, but there was no significant change at T<sub>3</sub> (Fig. 4E).

**Fig. 4** Effects of exosomes on ventricular muscle conduction velocity in IR model rats. (A) Conduction activation maps at T<sub>2</sub>. (B–D) Conduction velocity at T<sub>1</sub>, T<sub>2</sub>, and T<sub>3</sub>, n = 8, <sup>a</sup> P < 0.05, <sup>aa</sup> P < 0.01, <sup>aaaa</sup> P < 0.0001 vs IR; <sup>b</sup> P < 0.05, <sup>bbb</sup> P < 0.001 vs IR+ExoA, (E) Conduction velocity at each time point; <sup>c</sup> IR, <sup>cccc</sup> P < 0.0001 vs T<sub>1</sub>, <sup>d</sup> IR+ExoA, <sup>dddd</sup> P < 0.0001, <sup>eee</sup> P < 0.001 vs T<sub>1</sub>

#### ***Effect of exosome treatment on the distribution of Cx43 in left ventricular muscle of IR model rats***

Immunohistochemistry was used to stain Cx43 in the myocardial tissues of the model rats in each group (Fig. 5A). In the figure, the brown particles are Cx43 in the intercalated discs of the cardiomyocytes, and the blue particles are the nuclei of the cardiomyocytes. In the IR group, Cx43 protein expression was decreased, and its distribution was disordered. However, lateralization appeared to have occurred. Cx43 protein expression was higher in the IR+ExoB and IR+ExoA groups than in the IR group, and Cx43 expression in the IR+ExoB group was significantly higher than that in the IR+ExoA group, and the distribution was more orderly.

**Fig. 5** Effects of exosomes on Cx43 and myocardial injury. (A) Immunohistochemical staining of Cx43 in myocardial tissue of four group showing its expression levels and distribution, n = 3. (B) The expression of Cx43 in the myocardium of the four group by Western blotting, <sup>a</sup> P < 0.05, <sup>aaaa</sup> P < 0.0001 vs IR, <sup>bbb</sup> P < 0.001 vs IR+ExoA. (C) HE staining of myocardial injury in all groups. (D) Rats were injected with either DiR-Exo or vehicle (PBS) and analyzed after 30 min, 6 h, and 24 h. (E) Enrichment of exosomes in isolated hearts at 24 h after injection.

#### ***Effect of exosome pretreatment on the expression of Cx43 protein in ventricular muscle***

Western blotting of ventricular muscle tissue from IR model rats pretreated with exosomes or not showed that Cx43 protein expression in the C, IR+ExoB, and IR+ExoA groups was significantly higher than that in the IR group. Further, Cx43 protein expression levels were significantly higher in the IR+ExoB group than in the IR+ExoA group (Fig. 5B).

#### ***Effects of ischemia-reperfusion injury in each group***

HE staining showed that, in the control rats (C group), the myocardial fibers were arranged neatly, with clear myotomes and regular shapes. In contrast, in the IR group rats, cell swelling and increased vacuoles were observed. Some cardiomyocytes were disordered, with broken and wavy-curved myotomes. In the IR+ExoB group, cell swelling, uneven cytoplasmic staining, and myocardial arrangement were improved. Vacuolation was also decreased in the IR+ExoA group, but the improvement in myocardial fiber arrangement was not better than group IR+ExoB (Fig. 5C).

### *Distribution of C2C12-derived exosomes in rats*

The distribution of the injected exosomes in rats was observed by following injection of DiR-exo in PBS into the jugular veins of rats. At 30 min after injection, the fluorescence was weak and was mainly concentrated at the injection site. At 6 h after injection, the fluorescence was stronger. At 24 h after injection, the fluorescence was strongest, and it had spread to the abdomen. At this time point, the rats were anesthetized, and then their internal organs were dissected. Fluorescence imaging of the isolated heart showed that exosomes were enriched in the heart. No fluorescence was observed in the PBS-injected control rats at any time point. (Fig. 5D and E).

## **Discussion**

To explore whether exosomes are involved in the effect of RIPC on reperfusion arrhythmia, we subjected C2C12 myoblast cells to hypoxic preconditioning to simulate skeletal muscle RIPC. Our results showed that hypoxia preconditioning promoted the secretion of exosomes and significantly increased the number of exosomes, which is consistent with previous studies.

Exosomes contain numerous proteins, mRNAs, miRNAs, and lipids, and exosomes from different cell sources can carry different bioactive molecules to distal target cells and regulate their biological functions (Kalluri and Lebleu 2020; Lazo et al. 2021). Exosomes are important for substance exchange between cells and can be endocytosed or phagocytosed by recipient cells and degraded as nutrients by the lysosomes of the recipient cells (Kalluri and Lebleu 2020). Exosomes have a bilayer membrane structure with negative charge (-26mV) and express CD63 and other surface molecules. Exosomes have low immunogenicity and good membrane biocompatibility and can fuse with target cells to deliver functional bioactive molecules (Koritzinsky et al. 2017; Yang et al. 2020). These physiological characteristics facilitate their uptake by ischemic myocardial cells. Exosomes have been shown to be taken up by cardiomyocytes both in vitro and in vivo (Malik et al. 2013; Wang et al. 2016).

We hypothesize that the mechanism of RIPC myocardial protection (Heusch et al. 2015) may involve hypoxic stimulation of exosome production in large numbers. These exosomes reach cardiomyocytes through their communication functions and exert protective effects in the ischemic myocardium. In our study, live animal imaging of rats injected with DiR-labeled C2C12-derived exosomes into the jugular vein showed that the exosomes were enriched in the heart at 24 h after injection.

We established an isolated myocardial IR model in rats to examine ischemia-reperfusion arrhythmia and ventricular muscle conduction velocity after heartbeat restoration using a microelectrode array. Our results showed that the IR + ExoB group had a shorter cardiac relapse time, a lower arrhythmia score, and faster recovery of ventricular electrical activity than the IR group. In rats pretreated with hypoxia-preconditioned exosomes, conduction speed was higher, indicating better electrical conductivity. Therefore, hypoxia-pretreated exosomes improve ventricular conduction during ischemic reperfusion.

Previous studies by Mahoney et al. (2016) and our research team (Li et al. 2019a; Li et al. 2019b; Yi et al. 2022) showed that downregulation of Cx43 is related to decreased ventricular muscle conduction velocity in RA, and Cx43 has been detected on exosome membranes (Ribeiro-Rodrigues et al. 2017; Soares et al. 2015; Cho et al. 2021). In view of these findings, we compared Cx43 expression in the ventricular muscles of IR model rats pretreated with hypoxia-preconditioned exosomes and found that Cx43 expression was significantly higher in the ventricular muscles of rats in the hypoxia-preconditioned group than in the IR model and normoxic exosome pretreatment groups. This finding, combined the immunohistochemistry results, led us to speculate that exosomes may ameliorate myocardial reperfusion arrhythmias by promoting the expression of Cx43.

HE staining of the myocardia showed more obvious myocardial fiber rupture, cell swelling, and uneven staining in the IR group than in the IR+ExoA group and IR+ExoB group, which was consistent with the findings of Giricz et al. (Giricz et al. 2014; Lassen et al. 2021), indicating that extracellular vesicles are involved in cardiac protection mediated by distal ischemic preconditioning. These results suggest that hypoxia-preconditioned exosomes can reduce damage to ischemic myocardium.

Based on our results, we conclude that cardiac arrhythmia and electrical conduction in the IR+ExoB group were significantly better than in the IR and IR+ExoA groups, which may be due to the increase in exosomes generated in response to hypoxia preconditioning. However, this hypothesis requires confirmation in animal and clinical trials.

### **Limitations of the study**

This study has some limitations. We used hypoxia-preconditioned exosomes produced by C2C12 mouse myoblast cells to simulate the exosomes secreted following limb RIPC. As this is an in vitro mimic of RIPC, additional in vivo RIPC models and in vivo studies are required to determine the detailed mechanism of the remote protective functions conferred by RIPC. Our research group is currently investigating whether skeletal muscle-derived exosomes collected after RIPC have the same beneficial effect.

## **Conclusion**

Our results clearly show a change in the number of exosomes produced in response to hypoxia preconditioning as well as their positive effect on ischemia-reperfusion arrhythmias in isolated rat hearts. This shows that exosomes derived from C2C12 cells after hypoxia preconditioning could be involved in the mechanism delivering protective signals generated by RIPC in distant limbs to targeted tissues(Fig. 6). These findings provide a theoretical basis for a new promising strategy for the clinical improvement of myocardial ischemia-reperfusion arrhythmias.

## **Declarations**

### **Statements and Declarations**

## Data Availability

The datasets used and/or analyzed in this study are available from the corresponding authors upon reasonable request.

## Author Contributions

Tingju Hu and Rui Duan conducted experiments, collected data, and wrote the manuscript; Hong Gao was responsible for project conceptualization and design, and manuscript proofreading; Xue Bai, Xiang Huang, Rui Chen, Li An, Xu Yan, Yanyan Ma, Sen Hong, and Mi Gan conducted the experiments. All authors read and approved the final manuscript.

## Funding

This study was supported by the Science and Technology Fund of the Guizhou Provincial Health Commission (Grant No. Gzwkj2021-270).

## Competing Interests

All authors declare no conflict of interest.

## Acknowledgements

We thank Jianman Wang (College of Basic Medical College, Guizhou Medical University, Guiyang, Guizhou, China), Sihui Lu (College of Anesthesiology, Guizhou Medical University, Guiyang, Guizhou, China) and Anqiang Zhou (College of Clinic, Guizhou Medical University, Guiyang, Guizhou, China) for their kindful assistance with this study.

## References

1. AMANAKIS G, KLEINBONGARD P, HEUSCH G, et al. Attenuation of ST-segment elevation after ischemic conditioning maneuvers reflects cardioprotection online [J]. *Basic research in cardiology*, 2019, 114(3): 22.
2. AN L, GAO H, ZHONG Y, et al. The potential roles of stress-induced phosphoprotein 1 and connexin 43 in rats with reperfusion arrhythmia [J]. 2023, 11(10): e852.
3. BERNIKOVA O G, SEDOVA K A, ARTEYEVA N V, et al. Repolarization in perfused myocardium predicts reperfusion ventricular tachyarrhythmias [J]. *Journal of electrocardiology*, 2018, 51(3): 542–8.
4. CHEN K, WANG Q, LIU X, et al. Hypoxic pancreatic cancer derived exosomal miR-30b-5p promotes tumor angiogenesis by inhibiting GJA1 expression [J]. *International journal of biological sciences*, 2022, 18(3): 1220–37.
5. CHO H J, VELICHKOVSKA M, SCHURHOFF N, et al. Extracellular vesicles regulate gap junction-mediated intercellular communication and HIV-1 infection of human neural progenitor cells [J].

- Neurobiology of disease, 2021, 155(105388).
6. CHO Y J, KIM W H. Perioperative Cardioprotection by Remote Ischemic Conditioning [J]. International journal of molecular sciences, 2019, 20(19):
  7. DAVIDSON S M, FERDINANDY P, ANDREADOU I, et al. Multitarget Strategies to Reduce Myocardial Ischemia/Reperfusion Injury: JACC Review Topic of the Week [J]. Journal of the American College of Cardiology, 2019, 73(1): 89–99.
  8. DONATO M, BIN E P, V D A, et al. Myocardial remote ischemic preconditioning: from cell biology to clinical application [J]. Molecular and cellular biochemistry, 2021, 476(10): 3857–67.
  9. GAO R, WANG L, BEI Y, et al. Long Noncoding RNA Cardiac Physiological Hypertrophy-Associated Regulator Induces Cardiac Physiological Hypertrophy and Promotes Functional Recovery After Myocardial Ischemia-Reperfusion Injury [J]. Circulation, 2021, 144(4): 303–17.
  10. GIRICZ Z, VARGA Z V, BARANYAI T, et al. Cardioprotection by remote ischemic preconditioning of the rat heart is mediated by extracellular vesicles [J]. Journal of molecular and cellular cardiology, 2014, 68(75 – 8).
  11. GONCA E, DARICI F. The effect of cannabidiol on ischemia/reperfusion-induced ventricular arrhythmias: the role of adenosine A1 receptors [J]. Journal of cardiovascular pharmacology and therapeutics, 2015, 20(1): 76–83.
  12. HEUSCH G, BØTKER H E, PRZYKLENK K, et al. Remote ischemic conditioning [J]. Journal of the American College of Cardiology, 2015, 65(2): 177–95.
  13. HOU Z, QIN X, HU Y, et al. Longterm Exercise-Derived Exosomal miR-342-5p: A Novel Exerkine for Cardioprotection [J]. Circulation research, 2019, 124(9): 1386–400.
  14. IBÁÑEZ B, HEUSCH G, OVIZE M, et al. Evolving therapies for myocardial ischemia/reperfusion injury [J]. Journal of the American College of Cardiology, 2015, 65(14): 1454–71.
  15. KADRIC N, OSMANOVIC E. Rhythm Disturbance After Myocardial Revascularization [J]. Medical archives (Sarajevo, Bosnia and Herzegovina), 2017, 71(6): 400–3.
  16. KALLURI R, LEBLEU V S. The biology, function, and biomedical applications of exosomes [J]. Science (New York, NY), 2020, 367(6478):
  17. KHARBANDA R K, MORTENSEN U M, WHITE P A, et al. Transient limb ischemia induces remote ischemic preconditioning in vivo [J]. Circulation, 2002, 106(23): 2881–3.
  18. KINDERNAY L, FARKASOVA V, NECKAR J, et al. Impact of Maturation on Myocardial Response to Ischemia and the Effectiveness of Remote Preconditioning in Male Rats [J]. International journal of molecular sciences, 2021, 22(20):
  19. KLEINBONGARD P, BØTKER H E, OVIZE M, et al. Co-morbidities and co-medications as confounders of cardioprotection-Does it matter in the clinical setting? [J]. British journal of pharmacology, 2020, 177(23): 5252–69.
  20. KORITZINSKY E H, STREET J M, STAR R A, et al. Quantification of Exosomes [J]. Journal of cellular physiology, 2017, 232(7): 1587–90.

21. KULEK A R, ANZELL A, WIDER J M, et al. Mitochondrial Quality Control: Role in Cardiac Models of Lethal Ischemia-Reperfusion Injury [J]. *Cells*, 2020, 9(1):
22. LASSEN T R, JUST J, HJORTBAK M V, et al. Cardioprotection by remote ischemic conditioning is transferable by plasma and mediated by extracellular vesicles [J]. *Basic research in cardiology*, 2021, 116(1): 16.
23. LAZO S, NOREN HOOTEN N, GREEN J, et al. Mitochondrial DNA in extracellular vesicles declines with age [J]. *Aging cell*, 2021, 20(1): e13283.
24. LI W, GAO H, GAO J, et al. Upregulation of MMP-9 and CaMKII prompts cardiac electrophysiological changes that predispose denervated transplanted hearts to arrhythmogenesis after prolonged cold ischemic storage [J]. *Biomedicine & pharmacotherapy = Biomedecine & pharmacotherapie*, 2019, 112(108641).
25. LI W C, GAO H, GAO J, et al. Antiarrhythmic effect of sevoflurane as an additive to HTK solution on reperfusion arrhythmias induced by hypothermia and ischaemia is associated with the phosphorylation of connexin 43 at serine 368 [J]. *BMC anesthesiology*, 2019, 19(1): 5.
26. LUO Z, HU X, WU C, et al. Plasma exosomes generated by ischaemic preconditioning are cardioprotective in a rat heart failure model [J]. *British journal of anaesthesia*, 2023, 130(1): 29–38.
27. MA Y, CAO Y, GAO H, et al. Sevoflurane Improves Ventricular Conduction by Exosomes Derived from Rat Cardiac Fibroblasts After Hypothermic Global Ischemia-Reperfusion Injury [J]. *Drug design, development and therapy*, 2023, 17(1719–32).
28. MAHONEY V M, MEZZANO V, MIRAMS G R, et al. Connexin43 contributes to electrotonic conduction across scar tissue in the intact heart [J]. *Scientific reports*, 2016, 6(26744).
29. MALIK Z A, KOTT K S, POE A J, et al. Cardiac myocyte exosomes: stability, HSP60, and proteomics [J]. *American journal of physiology Heart and circulatory physiology*, 2013, 304(7): H954-65.
30. MINGHUA W, ZHIJIAN G, CHAHUA H, et al. Plasma exosomes induced by remote ischaemic preconditioning attenuate myocardial ischaemia/reperfusion injury by transferring miR-24 [J]. *Cell death & disease*, 2018, 9(3): 320.
31. OXMAN T, ARAD M, KLEIN R, et al. Limb ischemia preconditions the heart against reperfusion tachyarrhythmia [J]. *The American journal of physiology*, 1997, 273(4): H1707-12.
32. PATIL K D, HALPERIN H R, BECKER L B. Cardiac arrest: resuscitation and reperfusion [J]. *Circulation research*, 2015, 116(12): 2041–9.
33. PRZYKLENK K, BAUER B, OVIZE M, et al. Regional ischemic 'preconditioning' protects remote virgin myocardium from subsequent sustained coronary occlusion [J]. *Circulation*, 1993, 87(3): 893–9.
34. RIBEIRO-RODRIGUES T M, MARTINS-MARQUES T, MOREL S, et al. Role of connexin 43 in different forms of intercellular communication - gap junctions, extracellular vesicles and tunnelling nanotubes [J]. *Journal of cell science*, 2017, 130(21): 3619–30.
35. SOARES A R, MARTINS-MARQUES T, RIBEIRO-RODRIGUES T, et al. Gap junctional protein Cx43 is involved in the communication between extracellular vesicles and mammalian cells [J]. *Scientific reports*, 2015, 5(13243).

36. VICENCIO J M, YELLON D M, SIVARAMAN V, et al. Plasma exosomes protect the myocardium from ischemia-reperfusion injury [J]. *Journal of the American College of Cardiology*, 2015, 65(15): 1525–36.
37. WALKER M J, CURTIS M J, HEARSE D J, et al. The Lambeth Conventions: guidelines for the study of arrhythmias in ischaemia infarction, and reperfusion [J]. *Cardiovascular research*, 1988, 22(7): 447–55.
38. WANG G, DAI D, GAO H, et al. Sevoflurane Alleviates Reperfusion Arrhythmia by Ameliorating TDR and MAPD(90) in Isolated Rat Hearts after Ischemia-Reperfusion [J]. *Anesthesiology research and practice*, 2019, 2019(7910930).
39. WANG X, GU H, HUANG W, et al. Hsp20-Mediated Activation of Exosome Biogenesis in Cardiomyocytes Improves Cardiac Function and Angiogenesis in Diabetic Mice [J]. *Diabetes*, 2016, 65(10): 3111–28.
40. YAN Y, GU T, CHRISTENSEN S D K, et al. Cyclic Hypoxia Conditioning Alters the Content of Myoblast-Derived Extracellular Vesicles and Enhances Their Cell-Protective Functions [J]. *Biomedicines*, 2021, 9(9):
41. YAN Z, DU L, LIU Q, et al. Remote limb ischaemic conditioning produces cardioprotection in rats with testicular ischaemia-reperfusion injury [J]. *Experimental physiology*, 2021, 106(11): 2223–34.
42. YANG Z, SHI J, XIE J, et al. Large-scale generation of functional mRNA-encapsulating exosomes via cellular nanoporation [J]. *Nature biomedical engineering*, 2020, 4(1): 69–83.
43. YI J, DUAN H, CHEN K, et al. Cardiac Electrophysiological Changes and Downregulated Connexin 43 Prompts Reperfusion Arrhythmias Induced by Hypothermic Ischemia-Reperfusion Injury in Isolated Rat Hearts [J]. *Journal of cardiovascular translational research*, 2022, 15(6): 1464–73.

## Figures



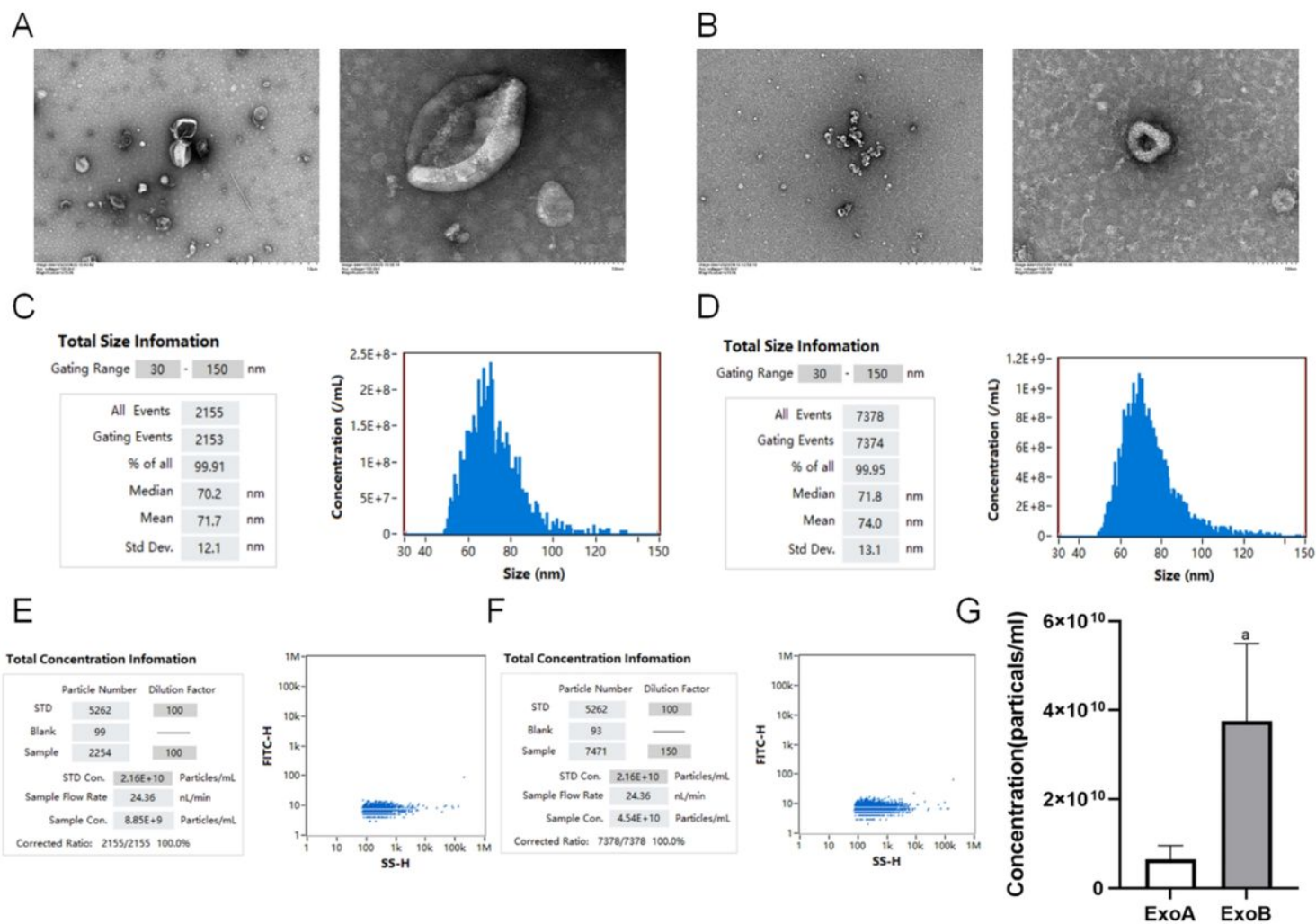


**Figure 1**

Identification and analysis of exosomes derived from normoxic (ExoA) and hypoxia-preconditioned (ExoB) C2C12 mouse myoblasts: (A, C, E) normoxic exosomes (ExoA) and (B, D, F) hypoxic-pretreated exosomes (ExoB). (G) Comparison of particle number between ExoA and ExoB,  $n = 3$ , <sup>a</sup>  $P < 0.05$  vs ExoA

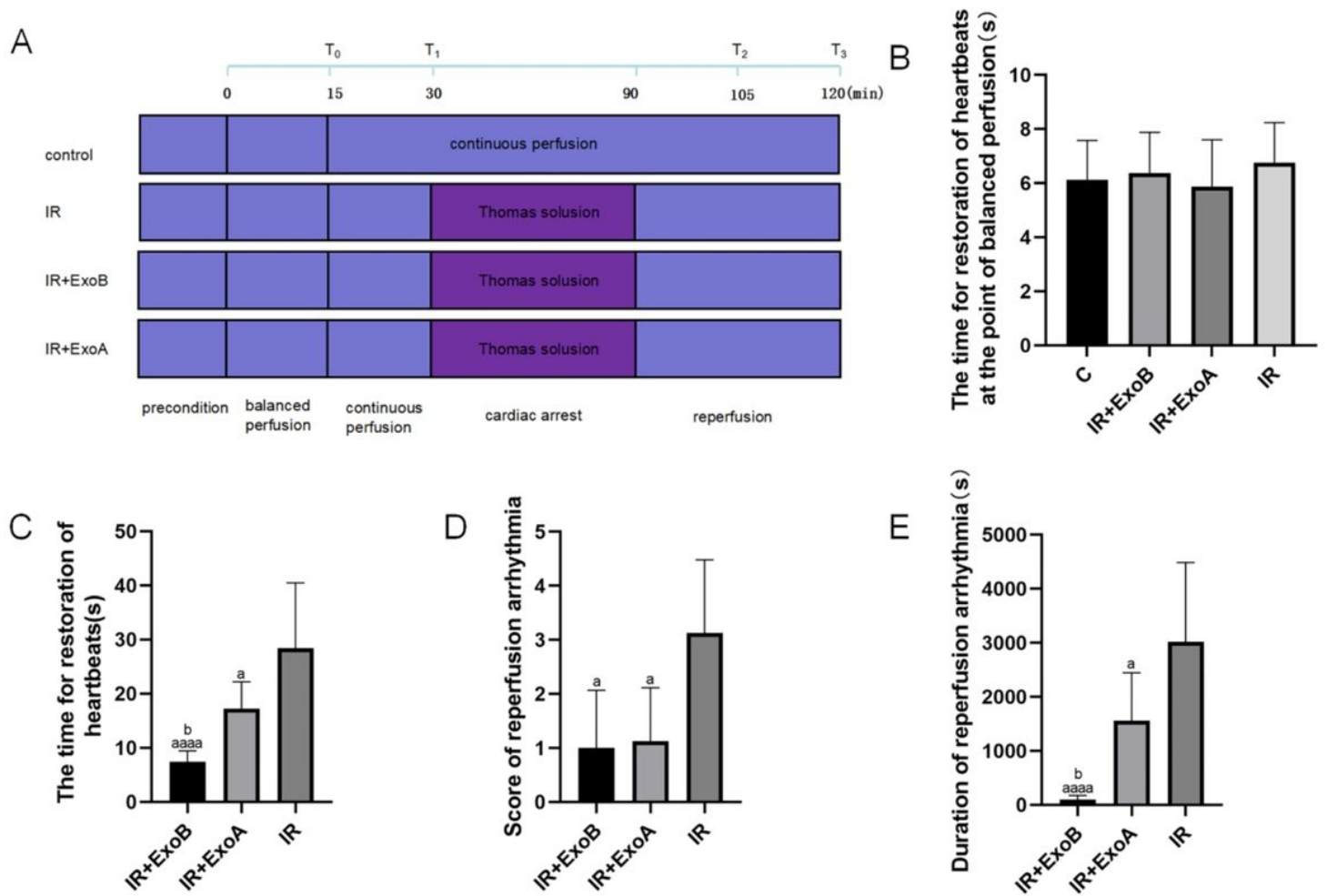


**Figure 2**

The effects of ExoB and ExoA to reperfusion arrhythmia. (A), Establishment of Langendorff isolated myocardial ischemia-reperfusion model rats (B), and analysis of the effects of exosomes on the time of heartbeat restoration during balanced perfusion (C), the time of heartbeat restoration during reperfusion (D), arrhythmia score (E), and the duration of reperfusion arrhythmia,  $n = 8$ ,  $^a P < 0.05$ ,  $^{aaaa} P < 0.0001$  vs IR;  $^b P < 0.05$  vs IR+ExoA

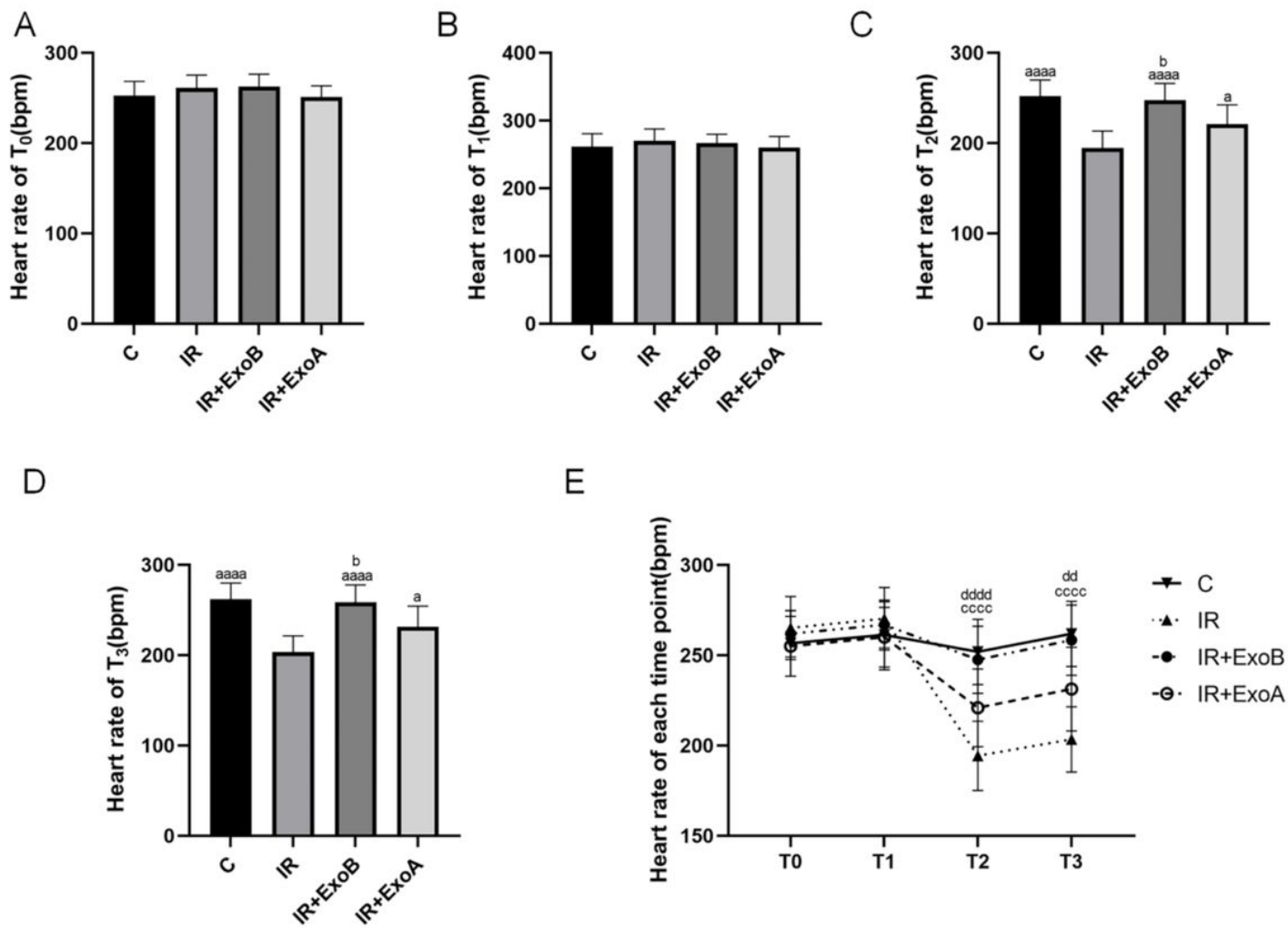


**Figure 3**

Effects of exosomes on the heart rate of model rats. (A–D) Heart rate at  $T_0$ ,  $T_1$ ,  $T_2$ , and  $T_3$ ,  $n = 8$ , <sup>a</sup>  $P < 0.05$ , <sup>aaaa</sup>  $P < 0.0001$  vs IR; <sup>b</sup>  $P < 0.05$  vs IR+ExoA, (E) Heart rate of all groups at each time point, <sup>c</sup> IR, <sup>cccc</sup>  $P < 0.0001$  vs  $T_1$ , <sup>d</sup> IR+ExoA, <sup>dd</sup>  $P < 0.01$ , <sup>dddd</sup>  $P < 0.0001$  vs  $T_1$

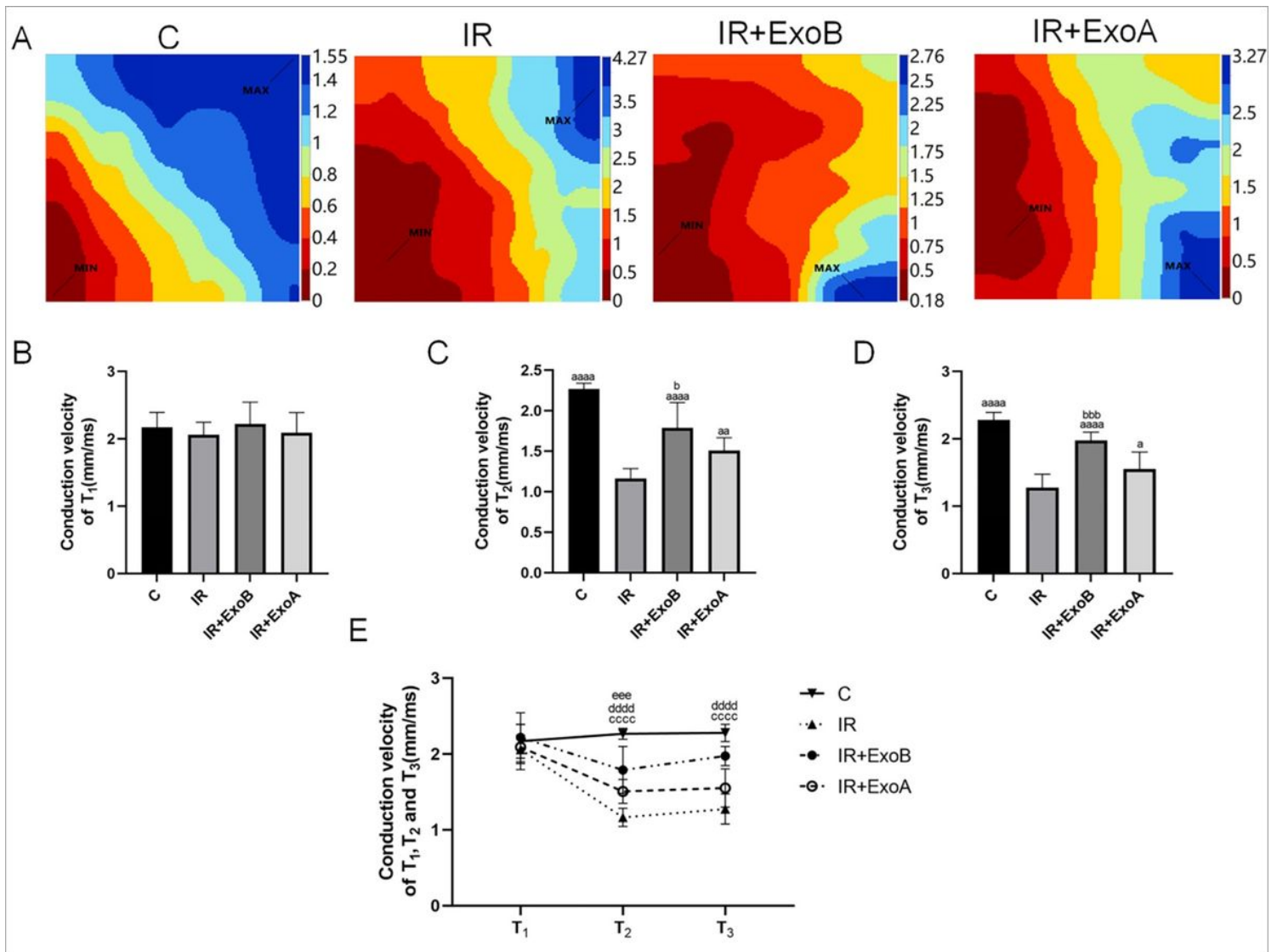


**Figure 4**

Effects of exosomes on ventricular muscle conduction velocity in IR model rats. (A) Conduction activation maps at T<sub>2</sub>. (B–D) Conduction velocity at T<sub>1</sub>, T<sub>2</sub>, and T<sub>3</sub>, n = 8, <sup>a</sup> P < 0.05, <sup>aa</sup> P < 0.01, <sup>aaaa</sup> P < 0.0001 vs IR; <sup>b</sup> P < 0.05, <sup>bbb</sup> P < 0.001 vs IR+ExoA, (E) Conduction velocity at each time point; <sup>c</sup> IR, <sup>cccc</sup> P < 0.0001 vs T<sub>1</sub>, <sup>d</sup> IR+ExoA, <sup>dddd</sup> P < 0.0001, <sup>eee</sup> P < 0.001 vs T<sub>1</sub>

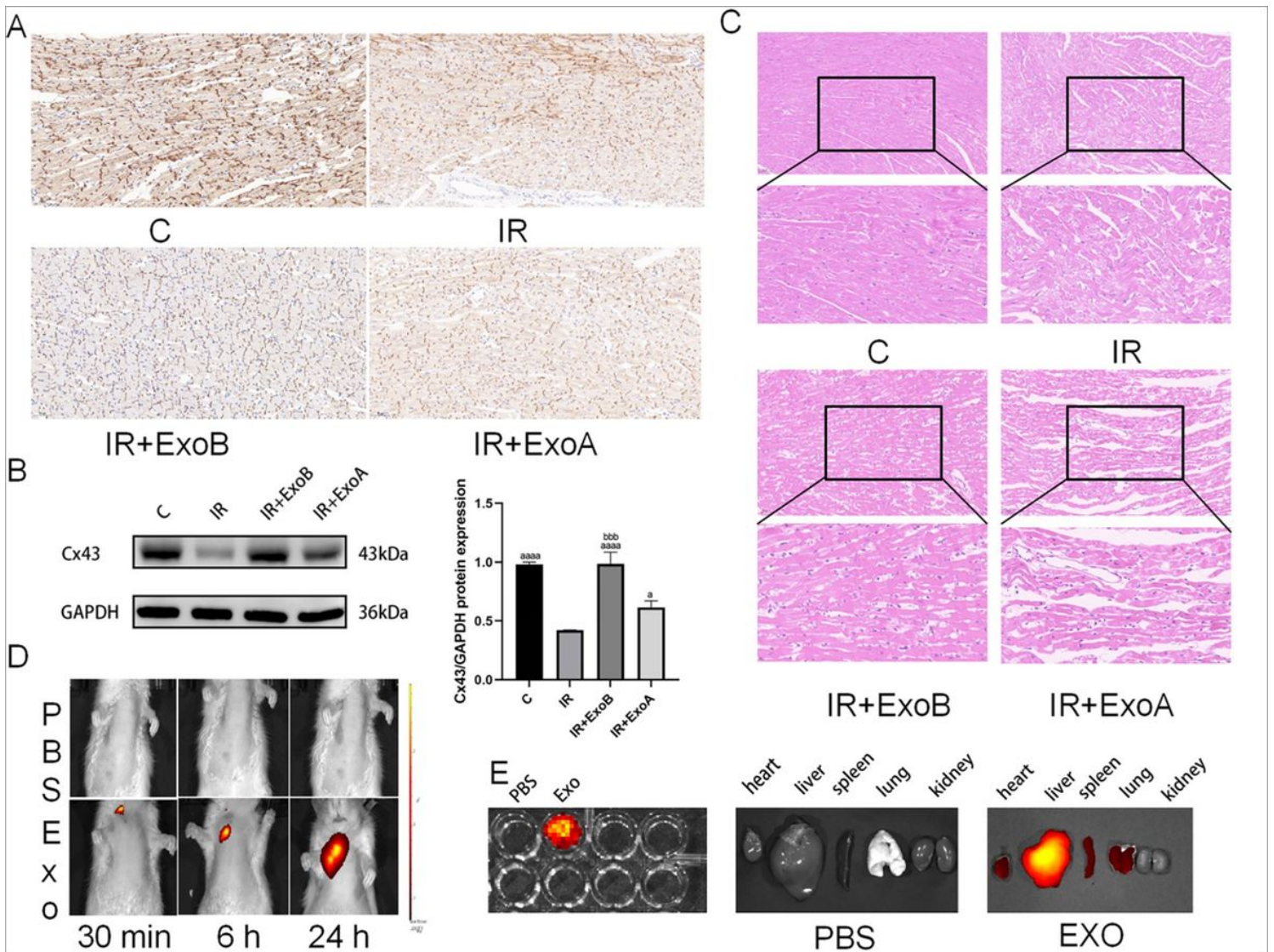


**Figure 5**

Effects of exosomes on Cx43 and myocardial injury. (A) Immunohistochemical staining of Cx43 in myocardial tissue of four groups showing its expression levels and distribution,  $n = 3$ . (B) The expression of Cx43 in the myocardium of the four groups by Western blotting, <sup>a</sup>  $P < 0.05$ , <sup>aaaa</sup>  $P < 0.0001$  vs IR, <sup>bbb</sup>  $P < 0.001$  vs IR+ExoA. (C) HE staining of myocardial injury in all groups. (D) Rats were injected with either DiR-Exo or vehicle (PBS) and analyzed after 30 min, 6 h, and 24 h. (E) Enrichment of exosomes in isolated hearts at 24 h after injection.

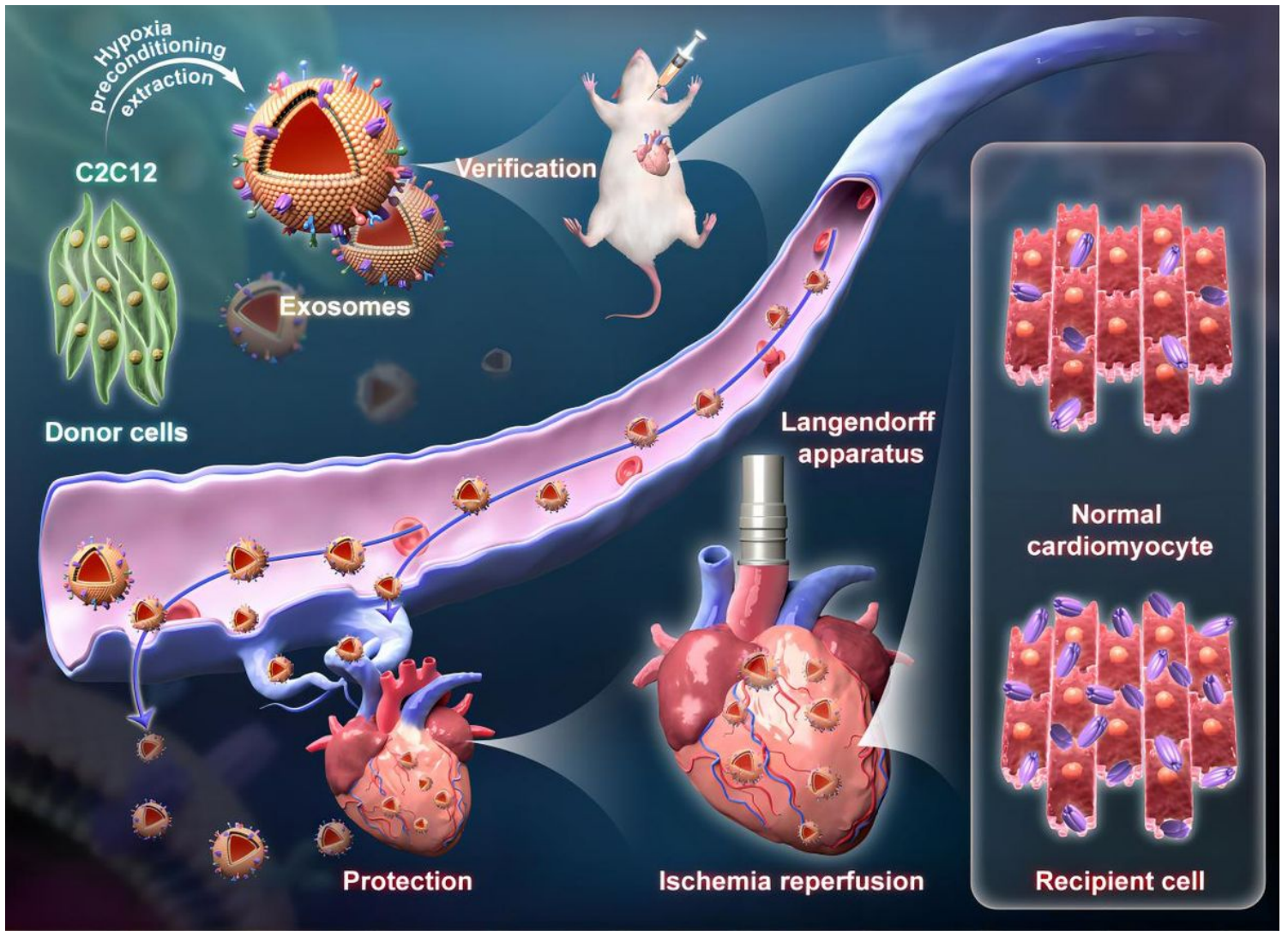


Figure 6

Graphical Abstract